2018 IEEE/RSJ International Conference on Intelligent Robots and Systems (IROS)
Madrid, Spain, October 1-5, 2018

Contact Force Control of an Aerial Manipulator in Pressing an Emergency Switch Process

Xiangdong Meng*, Yuqing He*, Qi Li, Feng Gu, Liying Yang, Tengfei Yan and Jianda Han

Abstract—**The dangerous work situation in industrial leakage accidents urgently needs a flexible and small robot to help workers perform operations and to protect them from being injured. An aerial manipulator system consisting of a hexa-rotor UAV and a one-DOF manipulator is developed, and is used to press an emergency switch to shut off machinery in an emergency. In practical application, an aerial manipulator usually performs contact operations as the UAV platform is in hover flight. The hovering UAV acting as a spring-mass-damper system is firstly proved. Then, based on the derived spring-mass-damper system model and the impedance control algorithm, the force-sensorless contact force control method is presented. That is, the force is indirectly controlled through controlling the UAV's position error and pitch angle simultaneously. The practical operation experiment of pressing an emergency button shows that the proposed method is able to control the contact force as the aerial manipulator interacts with the external environment.**

I. Introduction

When accidents happen in industrial production process, such as nuclear and toxic gas leakage [1, 2], the first response is to find the target and press an emergency stop button to shut down corresponding equipment quickly [3]. However, these situations are too dangerous for humans to enter, because of the potential for high radiation exposure or harmful effects on people eyes and respiration system. Therefore, there is a great need to develop a flexible and small robot for the emergency response to help workers fulfill this task and protect them from being injured.

An aerial manipulator, consisting of an unmanned aerial vehicle (UAV) and a one or multi degree-of-freedom (DOF) manipulator as shown in Fig. 1, is considered to be the best choice to perform these contact tasks, such as pressing an emergency stop switch in an emergency. This is because the system has many advantages listed in the following. Compared with ground mobile robots, aerial manipulators not only can move in 3-dimensional (3D) space, but also can perform operations in a high place as well as in the air. This kind of aircraft is small, flexible, and usually equipped with some sensors, which can avoid collisions and move freely even in a narrow space. Obstacles and corrosive liquids leaked from damaged pipes on the ground can be ignored for this aerial system, and it is easy to get into a workshop through a window if necessary [4]. Obviously, the application of an aerial manipulator in this situation is quite suitable. However, to use an aerial manipulator to perform contact operations still faces some challenging problems, one of which is the constant force control.

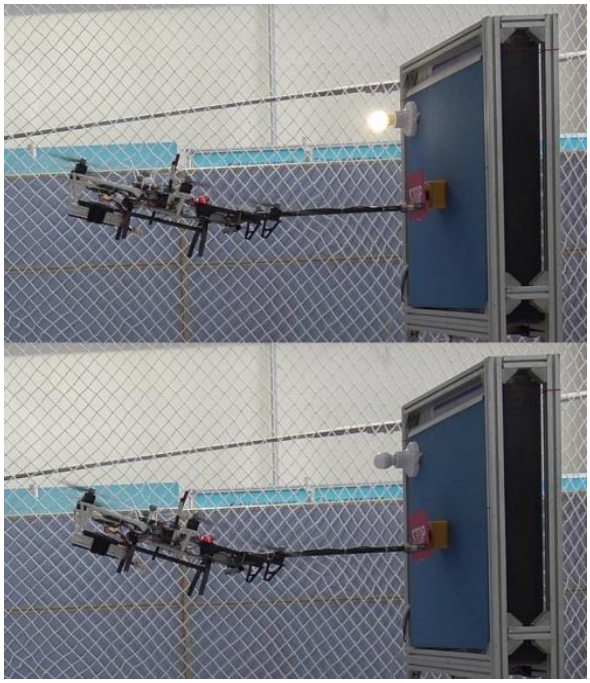

Figure 1. An aerial manipulator is pressing the emergency switch to turn off the light.

In recent years, the research of aerial manipulators has been a very popular field of study and achieved fruitful results. In [5], the aerial grasping of cylindrical object is realized by using visual servoing based on stochastic model predictive control. In [6], a local optimal trajectory planning method for an aerial manipulator is developed to obtain a collision-free trajectory for aerial operations. In [7], a human size dual arm aerial manipulator system is designed, and performs object

This work is supported by the National Natural Foundation of China (Grant Nos. 61433016 and 61503369), the Science Foundation of the Chinese Academy of Sciences (Grant No. 6141A01061601), the Youth Innovation Promotion Association of the Chinese Academy of Sciences and the Science and Technology Planning Project of Guangdong Province (Grant No. 2017B010116002).

Xiangdong Meng is Ph.D candidate at the State Key Laboratory of Robotics, Shenyang Institute of Automation, Chinese Academy of Sciences, Shenyang 110016, China & University of Chinese Academy of Sciences, Beijing 100049, China (e-mail: xdmeng09@gmail.com).

Yuqing He is with the State Key Laboratory of Robotics, Shenyang Institute of Automation, Chinese Academy of Sciences, Shenyang 110016 & Shenyang Institute of Automation (Guangzhou), Chinese Academy of Sciences, Guangzhou Guangdong 511458, China (e-mail: heyuqing@sia.cn).

Qi Li, Feng Gu, Liying Yang, Tengfei Yan and Jianda Han are all with the State Key Laboratory of Robotics, Shenyang Institute of Automation, Chinese Academy of Sciences, Shenyang 110016, China (e-mail: liqi, fenggu, yangliying, yantengfei, jdhan @sia.cn).

*Corresponding authors.

grasping with visual servoing. The aerial operation researches above are conducted as the aerial platform is in free flight condition. There are also some other works trying to control the aerial manipulator's contact force while its UAV platform's motion is constrained by its external environment. In [8], an LQR-optimized state feedback control algorithm is presented to control the substantial and sustained forces exerted on a vertical surfaces. In [9], by addition the output of force feedback into the desired position, the force control is integrated into the position control to achieve controlling the contact force, as the aerial manipulator is used in the bridge inspection task. In [10], an aerial manipulator system with a parallel robotic manipulator is designed for contact operations, and a passivity-based control law is used to track a fixed point and realize controlling the force of end-effector. An aerial manipulator consisting of a coaxial multirotor equipped with a robotic multi-link arm attached to the top of the multirotor body is developed for structure and bridge inspection [11], and the variable parameter integral back-stepping method is used to control the aerial manipulation vehicles.

In our research, as an aerial manipulator is performing contact operations, such as the task of pressing an emergency switch [12], the contact force in this process will be controlled. Then a force-sensorless contact force control strategy for the aerial manipulator is presented, which has been applied on the system as shown in Fig. 1. According to the practical features of aerial operations, an aerial manipulator usually performs contact tasks while the UAV platform is in hover flight or nearby. Additionally, plenty of experiments show that, with the help of a position control loop, a hover flying UAV behaves like a spring under an external force effect. That is, a certain external force exerting on a hovering UAV will cause the UAV deviates away from the desired hovering position, and after this external force disappears, the UAV's actual position will get back to the previous desired value. Based on this characteristic, our research controls the aerial manipulator to work as a spring-mass-damper system [13]. In addition, the idea of impedance control method is integrated into the process of contact force control, to realize controlling the force indirectly by controlling system position [14, 15]. In detail, the position error is controlled in order to control the contact force ultimately. From UAV's dynamics, it is known that under the effects of controllers a position error will cause an acceleration. And then the total system thrust will increase, in the meanwhile the corresponding desired attitude angles will appear to produce the rotation torques and to provide the component force for movement. That is to say, if the desired UAV's position error and attitude angle is given for the closed-loop UAV system according to the desired force, finally it will produce the corresponding desired control input for each rotor. At last, the UAV will maintain a certain thrust and corresponding attitude angle as it interacts with external environment. This process achieves the contact force control.

The paper is structured in the following manner. In Section II, an aerial manipulator system is developed for contact operations. Then in Section III, the hovering UAV acting as a spring-mass-damper system is proved theoretically, and the corresponding system model and characteristic analysis are given. In Section IV, based on the derived model and the impedance control algorithm, a force-sensorless contact force control method is presented. Next, the experiment of pressing an emergency switch is shown in Section V. Finally, the conclusion and our future work are introduced.

II. Aerial Manipulator System Description

A. System Structure

To perform the contact operation task, a one-DOF aerial manipulator system is designed to be lightweight and compact as shown in Fig. 2. Its aerial platform is a hexa-rotor UAV, which is commercial available. The employed autopilot is the Pixhawk open-source flight controller [16]. A link rod, made of carbon fiber tube, extends outside the rotor effect area to avoid the risk of collision, and also is used for operating purpose. In addition, a KingPROM ZHLBM-30 single axis force sensor is installed at the end of link rod to measure the force exerted on a target object. And the sensor can be interfaced with Pixhawk autopilot onboard via a data processing module. In order to contact the button firmly in the pushing process, a contact plate, also made of carbon fiber, is connected on the force sensor. A large torque JX servo is used to drive the link rod, providing a rotational degree of freedom for this one-DOF manipulator. A battery can be moved forward and back to balance the system center of gravity before taking off for stable flight. Some other basic system parameters are provided in TABLE I.

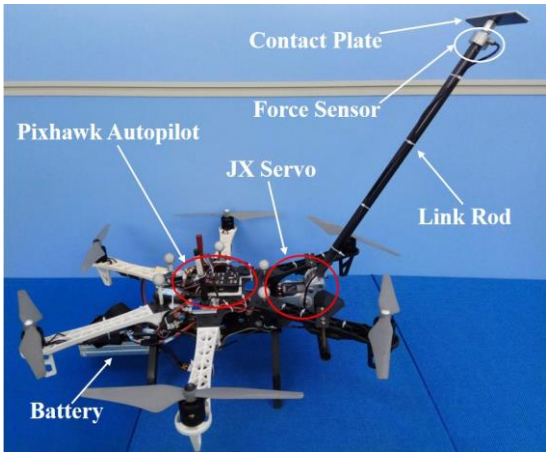

Figure 2. Aerial manipulator system introduction.

TABLE I. Main Parameters Of The Aerial Manipulator

Item	Value
Diagonal Wheelbase	550 mm
Propeller	9.4×5.0 inch
Link Rod Length	480 mm
Contact Plate	80 mm×20 mm
4 Cells Li-po Battery	395 g
Total Mass	2305 g
Moment of Inertia [I_x, I_y, I_z]	[0.0372, 0.0395, 0.062] kg.m^2

B. System Feature

The real-time force sensor data can be recorded by Pixhawk flight controller. In the process of contacting, if the exerted force exceeds a certain safety threshold, a warning will be sent

out on ground station for safe flight and operation. Additionally, the servo motor is designed to be automatically controlled by Pixhawk autopilot to compensate pitch angle in pushing button process as shown in Fig.1, keeping the manipulator link rod perpendicular to the wall, which also contributes to avoiding sliding motion on a vertical smooth surface.

III. System Model

In this session, the aerial manipulator acting as a spring-mass-damper system is firstly proved theoretically, and the corresponding system model and characteristic analysis are given in the next.

The definitions of inertial frame {I}, body-fixed frame {B}, and Euler angle $\boldsymbol{\Phi}=[\phi, \theta, \psi]$ are shown in Fig. 4. The position of the hexa-rotor in frame {I} is $\boldsymbol{p}=[x, y, z]$, the velocity is $\boldsymbol{v}=\dot{\boldsymbol{p}}$, the mass is m, the hexa-rotor arm length is l, the inertia matrix is $\boldsymbol{I}=diag\{[I_x, I_y, I_z]\}$, and the gravitational acceleration g is 9.81ms^{-2}. The UAV dynamics is presented as

$$\begin{cases} \ddot{x} = -u_1(\cos\phi\sin\theta\cos\psi + \sin\phi\sin\psi)/m \\ \ddot{y} = -u_1(\cos\phi\sin\theta\sin\psi - \sin\phi\cos\psi)/m \\ \ddot{z} = g - u_1\cos\phi\cos\theta/m \end{cases} \tag{1-a}$$

$$\begin{cases} \ddot{\phi} = a_2\dot{\theta}\dot{\psi} + b_2u_2 \\ \ddot{\theta} = a_3\dot{\phi}\dot{\psi} + b_3u_3 \\ \ddot{\psi} = a_4\dot{\phi}\dot{\theta} + b_4u_4 \end{cases} \tag{1-b}$$

where a_i and b_i are constants, $a_2 = (I_y - I_z)/I_x$, $a_3 = (I_z - I_x)/I_y$, $a_4 = (I_x - I_y)/I_z$, $b_2 = l/I_x$, $b_3 = l/I_y$, and $b_4 = 1/I_z$. u_1 is the UAV's thrust, u_2, u_3 and u_4 are torque inputs for each attitude axis. In order to study the hovering position response under external forces, UAV's attitude and altitude controllers are firstly designed, and then its horizontal position is controlled through inner-loop attitude dynamics, as shown in Fig. 3.

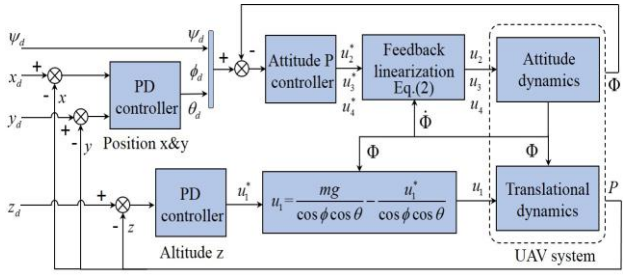

Figure 3. Control block diagram of UAV system.

A. Attitude Control

In the first, a feedback linearization is applied to UAV attitude dynamics in (1-b), the corresponding relationship between new virtual input variables u_2^*, u_3^*, u_4^* and the original variables u_2, u_3, u_4 are

$$\begin{cases} u_2 = (-a_2\dot{\theta}\dot{\psi} + k_2\dot{\phi})/b_2 + u_2^* \\ u_3 = (-a_3\dot{\phi}\dot{\psi} + k_3\dot{\theta})/b_3 + u_3^* \\ u_4 = (-a_4\dot{\phi}\dot{\theta} + k_4\dot{\psi})/b_4 + u_4^* \end{cases}. \tag{2}$$

As parameters k_2, k_3, $k_4 < 0$, UAV attitude dynamics can be guaranteed to be asymptotically stable. Then, a P controller $u_2^* = k_2^P(\phi_d - \phi)$ is applied and a second order transfer function for this closed-loop system can be acquired as

$$\frac{\phi(s)}{\phi_d(s)} = \frac{K_2^P}{s^2 - s\,k_2 + K_2^P},\quad K_2^P = b_2k_2^P. \tag{3}$$

In addition, the pitch and yaw transfer functions also can be obtained in the same way. By adjustment of the pair of parameters (k_2, k_2^P), (k_3, k_3^P), (k_4, k_4^P) respectively and with the only limitation k_2, k_3, $k_4 < 0$, the system desired dynamic performance can be achieved [17].

B. Position Control

For UAV's position control, its outputs are the desired throttle and desired attitudes. As the UAV is in hover flight, its altitude control output is approximately equal to the desired throttle, because of small accelerations in x and y horizontal position. By using variable substitution

$$u_1 = \frac{mg}{\cos\phi\cos\theta} - \frac{u_1^*}{\cos\phi\cos\theta},\quad \phi,\theta \neq \frac{\pi}{2}, \tag{4}$$

altitude dynamics in (1-a) is transformed as

$$m\ddot{z} = u_1^*. \tag{5}$$

Then, a PD controller $u_1^* = k_z^P(z_d - z) + k_z^D(\dot{z}_d - \dot{z})$ is applied and $\dot{z}_d$ is ignored as 0 for the hover flight. The relationship between UAV's actual altitude and the desired one is obtained as

$$\frac{z(s)}{z_d(s)} = \frac{k_z^P}{s^2m + sk_z^D + k_z^P}. \tag{6}$$

Similarly, by select appropriate parameters k_z^P and k_z^D, the desired altitude response can also be acquired.

Up to now, the UAV is able to realize stable flight in the air with the help of attitude controller and altitude controller. But, if a UAV is expected to be hovering at a certain position point in 3D space, the horizontal position controller is necessary.

For UAV's horizontal position control, its output is the desired attitude, which can be expressed as follows from (1-a)

$$\begin{aligned} \sin\phi_d &= -m\frac{u_x\sin\psi_d - u_y\cos\psi_d}{u_1} \\ \sin\theta_d &= -\frac{u_x m}{\cos\phi_d\cos\psi_d\,u_1} - \frac{\sin\phi_d\sin\psi_d}{\cos\phi_d\cos\psi_d} \end{aligned}, \tag{7}$$

where u_x and u_y are desired accelerations calculated from position PD controllers, as

$$\begin{aligned} u_x &= k_x^P(x_d - x) + k_x^D(\dot{x}_d - \dot{x}) \\ u_y &= k_y^P(y_d - y) + k_y^D(\dot{y}_d - \dot{y}) \end{aligned}. \tag{8}$$

As the UAV already can perform stable flight under attitude and altitude controllers, making its roll angle ϕ and pitch angle θ change in a small scale. In this case, the thrust u_1 in (4) is approximately equal to mg. And, to simplify the analysis, UAV's heading ψ is set to zero, leading to $\sin\psi = 0$, $\cos\psi = 1$. Meanwhile, the desired hover position can be anywhere in 3D space, so $(x_d, y_d, z_d) = (0, 0, 0)$ is all right. So the translational dynamics in (1-a) can be simplified into

$$\begin{aligned}\ddot{x} &= -g\theta \\ \ddot{y} &= g\phi\end{aligned}. \tag{9}$$

In addition, UAV's velocity approximately equals to zero as in hover flight, that is $\dot{x}_d$, $\dot{y}_d \approx 0$. Thus, from (8) and (9), equations in (7) are simplified as

$$\begin{aligned}\phi_d(s) &= (sK_y^D + K_y^P)y(s), \quad K_y^P = -k_y^P/g, K_y^D = -k_y^D/g \\ \theta_d(s) &= (sK_x^D + K_x^P)x(s), \quad K_x^P = k_x^P/g, K_x^D = k_x^D/g\end{aligned}. \tag{10}$$

So far, under the effects of attitude and position controllers, the UAV can perform stable hover flight at a certain 3D position point.

C. Closed-Loop Position Response under External Force

As a UAV or an aerial manipulator does operations in the environment, contact is inevitable. In this circumstance, the contact force effect is studied. Then, as an external force F_z^{ext} exerts on the z-axis, from (5) the relationship of altitude change can be obtained as

$$m\ddot{z} = k_z^P(z_d - z) - k_z^D\dot{z} + F_z^{ext}. \tag{11}$$

Beside, z_d is set to 0 as mentioned, then the altitude response under the external force is

$$z(s) = \frac{1}{s^2 m + sk_z^D + k_z^P} F_z^{ext}(s). \tag{12}$$

Similarly, when an external force F_x^{ext} exerts on the x-axis, or F_y^{ext} exerts on the y-axis, from (3), (9) and (10) the x and y position responses under external forces are presented as

$$x(s) = \frac{s^2 I_y - s k_3 I_y + l k_3^P}{s^2(s^2 I_y - s k_3 I_y + l k_3^P) + s l k_3^P k_x^D + l k_3^P k_x^P} \frac{F_x^{ext}(s)}{m}, \tag{13-a}$$

$$y(s) = \frac{s^2 I_x - s k_2 I_x + l k_2^P}{s^2(s^2 I_x - s k_2 I_x + l k_2^P) + s l k_2^P k_y^D + l k_2^P k_y^P} \frac{F_y^{ext}(s)}{m}. \tag{13-b}$$

The UAV is in position closed-loop condition and the external force changes slowly, which leads to a low frequency response of the system. Meanwhile, the aerial system is designed to be lightweight and compact, so its moment of inertia is smaller, as shown in TABLE I. Thus, the fractions (13) can be reduced to

$$x(s) = \frac{1}{s^2 m + sk_X^D + k_X^P} F_x^{ext}(s), \quad k_X^D = k_x^D m, k_X^P = k_x^P m, \tag{14-a}$$

$$y(s) = \frac{1}{s^2 m + sk_Y^D + k_Y^P} F_y^{ext}(s), \quad k_Y^D = k_y^D m, k_Y^P = k_y^P m. \tag{14-b}$$

D. Characteristic Analysis of Similar Spring-Mass-Damper System

From (12) and (14), it shows that the position response of a stable hovering UAV behaves like a spring-mass-damper system as shown in Fig. 4, no matter it is altitude or horizontal position [13]. The altitude controller parameters k_z^P and k_z^D, and the horizontal position controller parameters k_x^P, k_x^D, k_y^P and k_y^D can be considered as the spring-mass-damper system stiffness and damping on the corresponding axis, and the whole UAV mass is its mass. Meanwhile, the system stiffness and damping can also be adjusted by selecting appropriate parameters for each controller.

***Remark*:** An aerial manipulator is able to perform many contact tasks, and the contact force in the operation process is ultimately provided by the UAV platform. Therefore, according to the characteristics of different aerial operations, these UAV's controller parameters can be adjusted to acquire the desired platform stiffness and damping, which contributes to a satisfactory result.

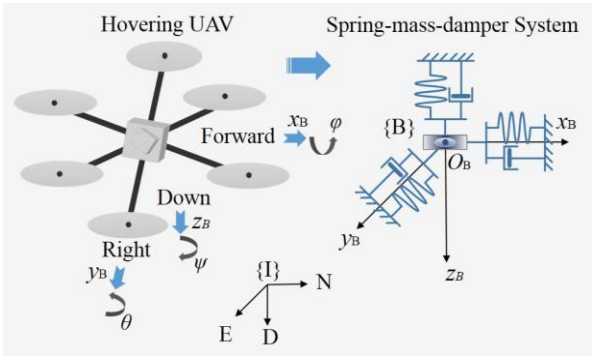

Figure 4. A hovering UAV acts as a spring-mass-damper system.

In addition, just like an ordinary spring, this system has the same characteristics. An external force exerting on it will lead to a displacement, and in contrast a displacement deviating from the equilibrium position will cause a corresponding force. This feature will be applied on the contact force control in next section.

IV. Contact Force Control

As an aerial manipulator performs contact tasks, such as the operation of pressing an emergency switch, the contact force in the process has to be controlled and sometimes needs to be maintained for a while. The impedance control technique proposed by Hogan is one of the fundamental approaches for force tracking control of robot manipulators with constrained motion [14, 15]. Impedance control regulates the force between a manipulator and the environment by defining the target impedance between position and contact force. The desired force is indirectly controlled by pre-specifying a robot positional reference trajectory that is determined based on the stiffness and location of the environment [18]. This impedance control idea will be used in the process of aerial manipulator contact force control.

No matter what kind of aerial platform it is, one of the most basic premise is that this system can achieve stable and reliable flying in the air. Therefore, the aerial manipulator system control has two purposes: one is stabilizing the UAV platform, and the other is to realize the contact force control. The UAV already has attitude and position closed-loop controllers, which contributes to achieving the first goal.

As to the second, the contact force control can be realized by using the impedance control idea. A UAV system has four inputs to control motor rotation in order to produce the aerodynamic force and moment. From UAV's dynamics (1), it is known that under the effects of controller a position error will cause an acceleration. And then the total system thrust

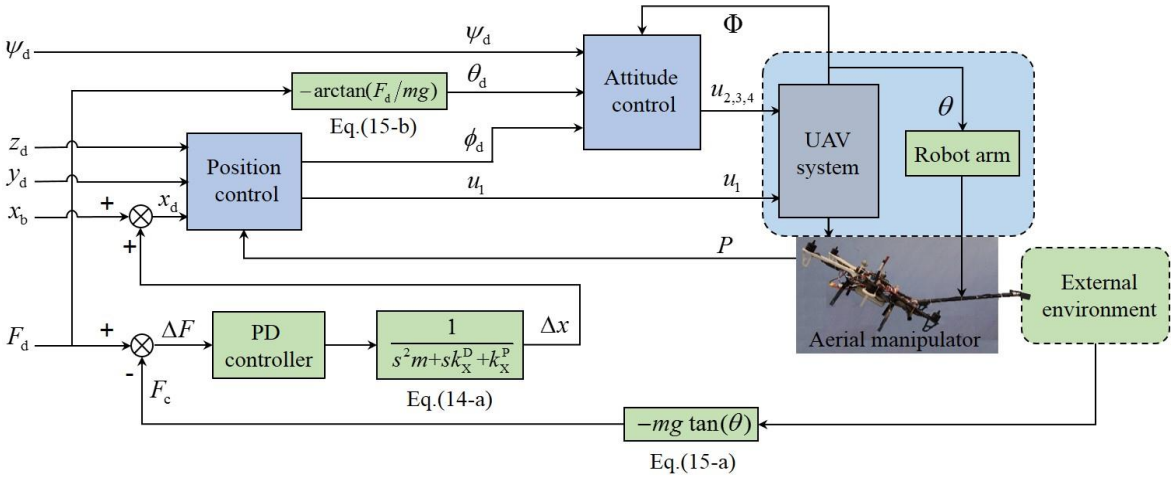

Figure 6. Contact force control block diagram of aerial manipulator.

will increase, in the meanwhile the corresponding desired attitude angles (especially the pitch and roll angle) will appear to produce the rotation torques and to provide the component force for movement [8, 9, 19]. That is to say, if the desired UAV's position error and attitude angle is given for the closed-loop UAV system according to the desired force, finally it will produce the corresponding desired control inputs u_1~u_4. In this way, as the UAV is in a constrained environment there will be a force applying on the contacting object or it will contribute to an acceleration as the UAV is in free flight. The whole process above is just the application of the impedance control idea. It can achieve controlling aerial manipulator contact force, and in the same time the aerial platform can also maintain a stable and reliable flight while it interacts with the environment.

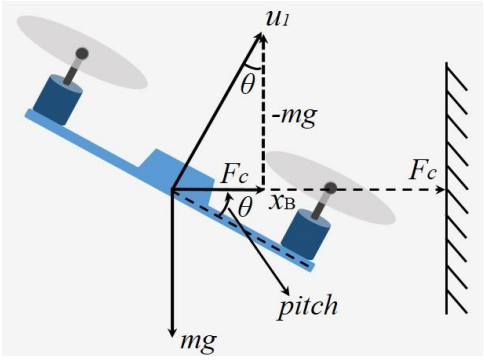

Figure 5. Relationships among contact force, thrust and gravity force.

In this research, the aerial manipulator contact force control in the forward direction is studied. When a UAV is contacting the environment with a certain pitch angle, the relationships among the contact force F_c, the throttle thrust u_1 and its gravity mg can be found in Fig. 5, as

$$F_c = -mg\tan(\theta), \tag{15-a}$$

$$\theta_d = -\arctan(F_d/mg). \tag{15-b}$$

The contact force F_c, a perpendicular force to the vertical surface, can be calculated from (15-a) without using a force sensor, but the UAV acts as the sensor in this circumstances. In the meanwhile, the desired pitch angle can also be obtained from desired contact force and system gravity as in (15-b). The key point of the proposed method is controlling position error in order to control the contact force ultimately. That is, the UAV's position error $\Delta X = x_d - x_b$ is controlled to realize controlling the contact force, in which x_d is the desired position and x_b is the body actual position of aerial platform. Although UAV's actual position is hard to change because of the limitation of external environment, its desired position can be set arbitrarily. In this way, its position error can be modified to produce the desired throttle as a certain contact force is controlled.

Based on impedance control idea and the above derived spring-mass-damper system model, the UAV's position error is controlled to realize control the contact force, and its force control block diagram is shown in Fig. 6. The contact force is controlled by a PD controller, and the corresponding micro displacement Δx can be calculated from force error Δy by (14-a). Additionally, the servo is designed to be automatically controlled by Pixhawk autopilot to compensate pitch angle to ensure that the contact force is perpendicular to the vertical surface, which is also easily for pressing an emergency switch button.

V. Experiment

The proposed contact force control algorithm has been implemented on the aerial manipulator system for the operation of pressing an emergency switch. In this experiment, a commercially available emergency stop switch, the yellow one shown in Fig. 1, is screwed on a vertical board, which is about 1.5 m above the ground. A 10×10 cm plastic board, the red one shown in Fig. 1, is stuck on the switch button for contacting, for the original button diameter is only about 4 cm and too small for operation. As mentioned, the emergency stop button is used to shut off machinery in an emergency, which is the light in the experiment. So, this light will be turned off as the emergency stop button is pressed down.

The experiment is carried out in the Motive motion capture system, which provides position information indoors [20]. The whole operation process is divided into several steps:

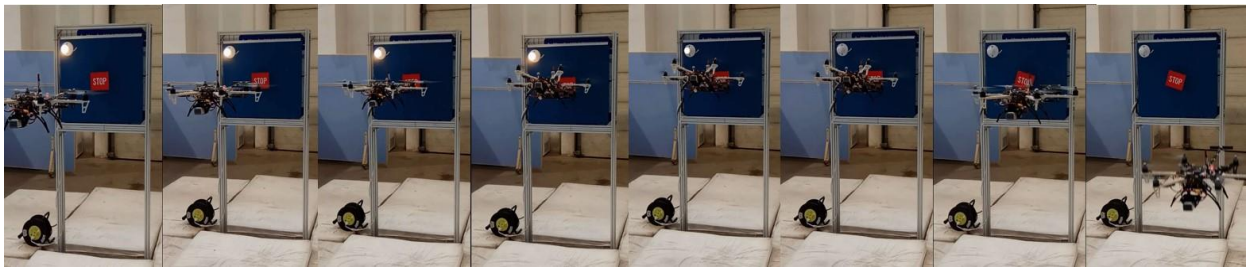

(a) Front view

(b) Side view

Figure 7. The process of pressing an emergency switch with the aerial manipulator system.

taking-off, approaching target, contacting target, contact force control, return and landing, as shown in Fig. 7. Among these steps, taking-off, return and landing can be controlled automatically or by remote control. But, approaching target, contacting target and contact force control must rely on controller to avoid failure and danger.

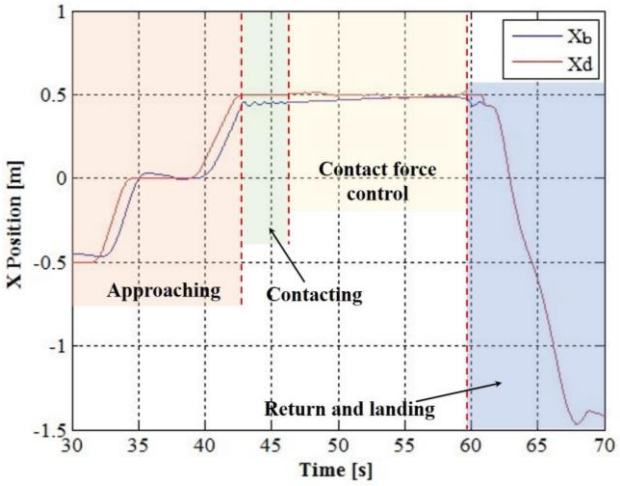

Figure 8. The real-time X position of aerial manipulator.

The onboard force sensor is only used to measure the contact force in the process. The aerial manipulator system takes off manually and is hovering at the position (-0.5m, 0, 1.5m), which is about 1 m in front of the emergency switch, as shown in Fig. 8. Then, it approaches and contacts with the button automatically. In the contacting process, the force and vibration will appear and reach maximum at the moment of contact, and then decrease gradually as shown in Fig. 9. As the vibration disappears, the contact force is controlled to reach the desired value for pressing the button. Note that the emergency switch has been already tested by a force sensor, and a 6.5N force is able to press down the button successfully. Therefore, a desired ramp force $F_d = 1\text{N/s}\cdot t$, $(0<t<7)$, with the final value 7 N, is tracked for the pressing task, as the red curve shown in Fig. 9. After the button is pressed down and light is turned off successfully, the aerial manipulator returns and lands manually. The experiment result shows the operation process in the range from 30s to 70s.

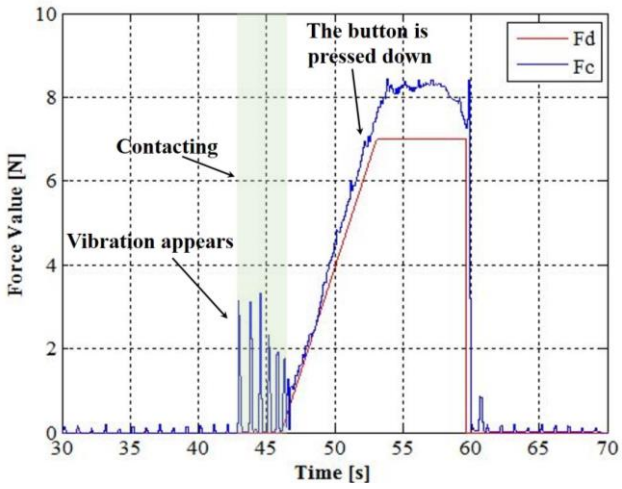

Figure 9. The measured contact force and desired force.

The goal of this experiment is to press down the emergency switch efficiently in a short time, and there exists a force tracking error shown in Fig. 9, in which the desired final force is 7N and the actual measured value is 8.1N. This is because a small overshoot exists in the pitch angle tracking process as shown in Fig. 10. This attitude overshoot is hardly eliminated by adjusting the attitude controller parameters merely, for the large parameters will cause system oscillation. However, some predictive method can be used to compensate attitude vibration in contact operation process to obtain the accurate force tracking.

The key problem in the button pressing process is the contact force control. The force is indirectly controlled

through controlling the position error and corresponding pitch angle simultaneously. Thus, the total thrust and pitch angle are two important system status for the safe and reliable aerial operation, which are shown in Fig. 11 and Fig. 10 respectively. And the thrust is kept on a steady value as the constant desired contact force is controlled as shown in Fig .11.

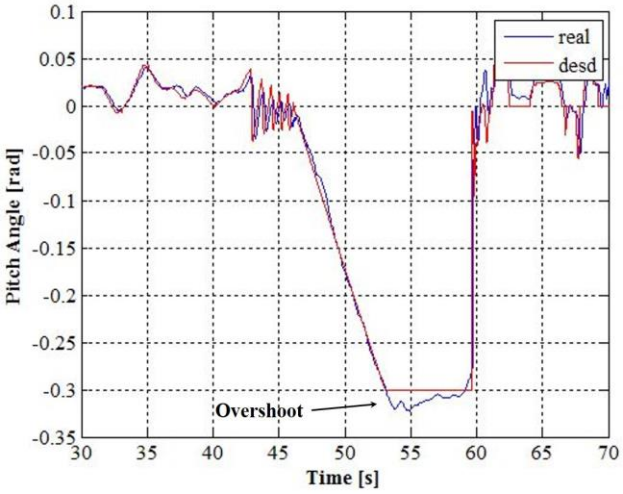

Figure 10. The pitch angle states of UAV in the operation process.

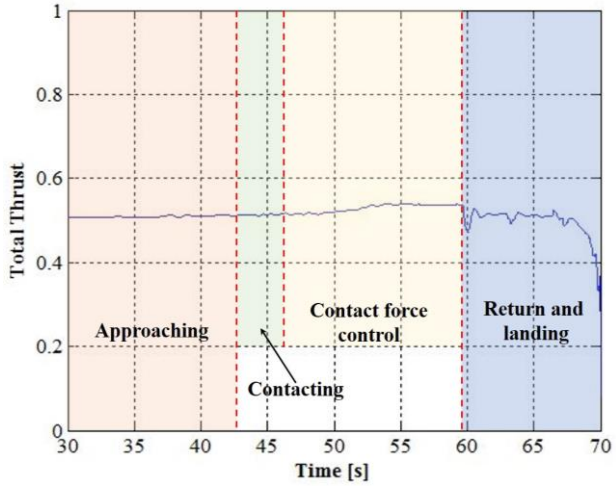

Figure 11. The total thrust of aerial platform in the operation.

The attached video to this paper shows the performed experiments, as described in this Section.

VI. CONCLUSION

In this paper, an aerial manipulator system consisting of a hexa-rotor UAV and a one-DOF manipulator is introduced for pressing an emergency switch in an emergency. The hovering UAV acting as a spring-mass-damper system has been proved. Based on impedance control algorithm and the derived spring-mass-damper system model, the contact force control method is presented. The factual operation of pressing an emergency button is conducted automatically. And the experiment result shows that the proposed force control method is able to control the contact force as interacting with external environment. In addition, considering the aerial manipulator is expected to fulfill complex tasks in unstructured environment in the future, the more DOF aerial manipulator and environment perception are necessary in our future work.

REFERENCES

[1] Visschers V H M, Siegrist M, "How a nuclear power plant accident influences acceptance of nuclear power: Results of a longitudinal study before and after the Fukushima disaster," Risk analysis, vol. 33:2, pp. 333-347, 2013.

[2] Ruj B, Chatterjee P K, "Toxic release of chlorine and off-site emergency scenario–A case study," Journal of Loss Prevention in the Process Industries, vol. 25:3, pp. 650-653, 2012.

[3] https://en.wikipedia.org/wiki/Kill_switch.

[4] Falanga D, Mueggler E, Faessler M, et al., "Aggressive quadrotor flight through narrow gaps with onboard sensing and computing using active vision," Robotics and Automation (ICRA), 2017 IEEE International Conference on, pp. 5774-5781, 2017.

[5] Seo H, Kim S, Kim H J., "Aerial grasping of cylindrical object using visual servoing based on stochastic model predictive control," Robotics and Automation (ICRA), 2017 IEEE International Conference on, pp. 6362-6368, 2017.

[6] Seo H, Kim S, Kim H J., " Locally optimal trajectory planning for aerial manipulation in constrained environments," Intelligent Robots and Systems (IROS), 2017 IEEE/RSJ International Conference on., pp. 1719-1724, 2017.

[7] Suarez A, Soria P R, Heredia G, et al., "Anthropomorphic, compliant and lightweight dual arm system for aerial manipulation," Intelligent Robots and Systems (IROS), 2017 IEEE/RSJ International Conference on., pp. 992-997, 2017.

[8] Wopereis H W, Hoekstra J J, Post T H, et al., "Application of substantial and sustained force to vertical surfaces using a quadrotor," Robotics and Automation (ICRA), 2017 IEEE International Conference on., pp. 2704-2709, 2017.

[9] Ikeda T, Yasui S, Fujihara M, et al., "Wall contact by octo-rotor UAV with one DoF manipulator for bridge inspection," Intelligent Robots and Systems (IROS), 2017 IEEE/RSJ International Conference on., pp. 5122-5127, 2017.

[10] Macchelli A, Forte F, Keemink A Q L, Stramigioli S, et al. "Developing an aerial manipulator prototype," IEEE Robotics and Automation Magazine, vol. 21:3, pp. 41-55, 2014.

[11] Jimenez-Cano A E, Braga J, Heredia G, et al., "Aerial manipulator for structure inspection by contact from the underside," Intelligent Robots and Systems (IROS), 2015 IEEE/RSJ International Conference on., pp. 1879-1884, 2015.

[12] Kim S, Lee G., "Haptic feedback design for a virtual button along force-displacement curves," Proceedings of the 26th annual ACM symposium on User interface software and technology, pp. 91-96, 2013.

[13] Lakhlani B, Yadav H, "Development and analysis of an experimental setup of spring-mass-damper system," Procedia Engineering, vol. 173, pp. 1808-1815, 2017.

[14] Hogan N., "Stable execution of contact tasks using impedance control," Robotics and Automation. Proceedings. 1987 IEEE International Conference on., pp. 1047-1054, 1987.

[15] Hogan N., "Impedance control: An approach to manipulation: Part II—Implementation," Journal of dynamic systems, measurement, and control, vol. 107: 1, pp. 8-16, 1985.

[16] https://pixhawk.org & http://px4.io.

[17] Meng X, He Y, Gu F, et al.,"Dynamics modeling and simulation analysis for rotorcraft aerial manipulator system," Control Conference (CCC) 36th Chinese, pp. 1156-1161, 2017.

[18] Jung S, Hsia T C, Bonitz R G., "Force tracking impedance control for robot manipulators with an unknown environment: theory, simulation, and experiment," The International Journal of Robotics Research, vol. 20: 9, pp. 765-774, 2001.

[19] Kendoul F, Yu Z, Nonami K., "Guidance and nonlinear control system for autonomous flight of minirotorcraft unmanned aerial vehicles," Journal of Field Robotics, vol. 27: 3, pp. 311-334, 2010.

[20] http://www.optitrack.com/applications/